

## Measurement-Induced Transition in Long-Range Interacting Quantum Circuits

Maxwell Block<sup>1</sup>, Yimu Bao<sup>1</sup>, Soonwon Choi<sup>1,2</sup>, Ehud Altman<sup>1,3</sup>, and Norman Y. Yao<sup>1,3</sup><sup>1</sup>*Department of Physics, University of California, Berkeley, California 94720, USA*<sup>2</sup>*Center for Theoretical Physics, Massachusetts Institute of Technology, Cambridge, Massachusetts 02139, USA*<sup>3</sup>*Materials Sciences Division, Lawrence Berkeley National Laboratory, Berkeley, California 94720, USA*

(Received 14 May 2021; accepted 2 November 2021; published 5 January 2022)

The competition between scrambling unitary evolution and projective measurements leads to a phase transition in the dynamics of quantum entanglement. Here, we demonstrate that the nature of this transition is fundamentally altered by the presence of long-range, power-law interactions. For sufficiently weak power laws, the measurement-induced transition is described by conformal field theory, analogous to short-range-interacting hybrid circuits. However, beyond a critical power law, we demonstrate that long-range interactions give rise to a continuum of nonconformal universality classes, with continuously varying critical exponents. We numerically determine the phase diagram for a one-dimensional, long-range-interacting hybrid circuit model as a function of the power-law exponent and the measurement rate. Finally, by using an analytic mapping to a long-range quantum Ising model, we provide a theoretical understanding for the critical power law.

DOI: 10.1103/PhysRevLett.128.010604

Programmable simulators—capable of supporting many-body entanglement—have opened the door to a new family of quantum dynamical questions [1–6]. A unifying theme behind these queries is the competition between many-body entangling interactions and entanglement-suppressing dynamics. For example, many-body localization arises when interactions are pitted against strong disorder [7–10]. Similarly, the dissipative preparation of entangled states requires a delicate balance between unitary and incoherent evolution [11–15]. Recently, a tremendous amount of excitement has focused on a new paradigm for such competition, namely, “hybrid” quantum circuits composed of scrambling dynamics interspersed with projective measurements (Fig. 1) [16,18–22].

Naively, such evolution appears similar to the perhaps more familiar case of open-system dynamics, where an environment is viewed as constantly measuring the system. But there is a crucial difference: in open-system dynamics, the results of the environment’s measurements are unknown, and only the average over outcomes determines the system’s evolution [23–25]. In hybrid quantum circuits, however, the projective measurement results are recorded, so the dynamics resolve individual quantum trajectories [18,20]. This distinction has a profound consequence on the long-time dynamics.

Most fundamentally, instead of approaching a steady-state density matrix, the system perpetually fluctuates in Hilbert space, building up many-body entanglement that is, possibly, later eradicated by a few well-placed measurements [26–31]. This constant ebb and flow of entanglement gives rise to a novel dynamical phase transition: at low measurement rates, the dynamics generate extensive

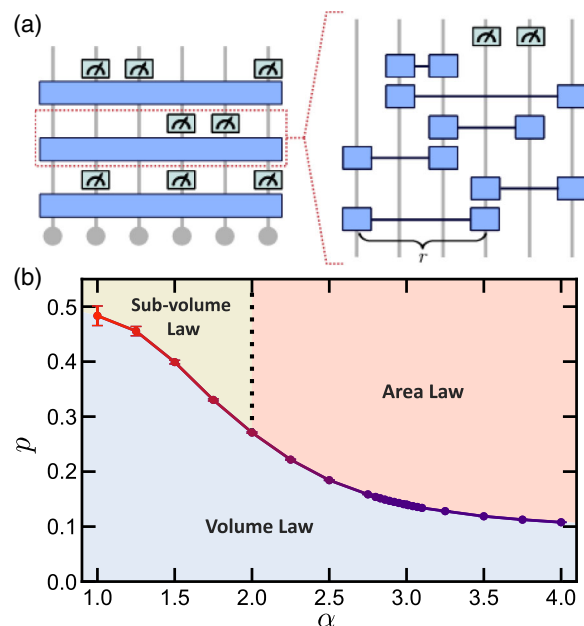


FIG. 1. (a) Schematic of our long-range interacting hybrid circuit, which consists of layers of unitary evolution and randomly placed projective measurements. Two-qubit gates separated by distance  $r$  occur with a probability  $P(r) \sim 1/r^\alpha$ . (b) Phase diagram as a function of the measurement rate  $p$  and the power-law exponent  $\alpha$ . For  $\alpha \gtrsim 3$ , the measurement-induced phase transition is described by conformal field theory (purple), while for  $\alpha \lesssim 3$ , the universality changes continuously (purple-red gradient). For  $\alpha < 2$ , area-law entropy scaling crosses over to subvolume law scaling, where half-chain entanglement entropy ( $S_{L/2}$ ) scales as  $L^{2-\alpha}$ . Despite this different scaling behavior, both the area and subvolume law regimes are in the purifying phase.

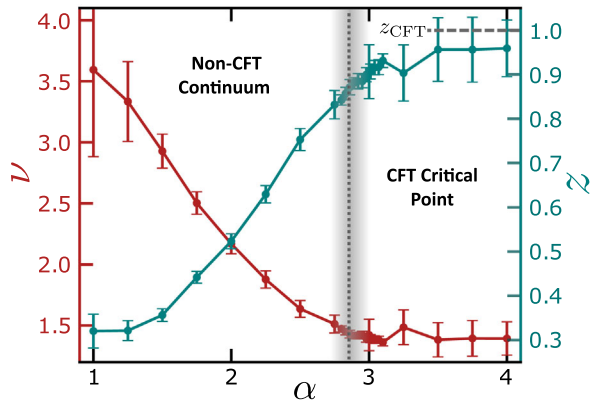


FIG. 2. The correlation length critical exponent,  $\nu$  (red), and the dynamical critical exponent,  $z$  (teal), extracted from a finite-size scaling analysis of the purification time. For  $\alpha \gtrsim 3$ , one finds  $z \approx 1$  corresponding to CFT. For  $\alpha \lesssim 3$ , both critical exponents vary continuously, indicating a continuum of non-CFT universality classes in this regime. The dotted line (and shaded grey region) is consistent with a critical power law,  $\alpha_c = 3 - \eta$ , where  $\eta \sim 0.2$  is the anomalous dimension.

entanglement, while at high measurement rates, only few-body entangled clusters emerge [18–20]. To date, this measurement-induced transition has been explored in two limits: hybrid quantum circuits with local interactions [30,32–37] and all-to-all interacting circuits where powerful analytic techniques can be applied [38–40]. Understanding the nature of the measurement-induced transition in generic, long-range-interacting systems (i.e., with power laws  $\sim 1/r^\alpha$ ) remains an essential open question that finds motivation from two complementary angles.

First, such long-range interactions are known to have profound effects on the universality, and indeed, even the existence, of many phase transitions [41–46]; in addition, long-range interactions can parametrically alter the form of Lieb-Robinson bounds and scrambling light cones [47–50]. Second, many of the most promising experimental platforms for investigating the measurement-induced transition, including Rydberg tweezer arrays, polar molecules, trapped ions and solid-state magnetic dipoles, inherently feature long-range interactions [51–55].

In this Letter, we demonstrate that the interplay between long-range interactions and projective measurements leads to fundamentally new universality classes for the measurement-induced transition. Our main results are threefold. First, we find that for  $\alpha \gtrsim 3$  the universality class is consistent with previous studies of short-range models; however, for  $\alpha \lesssim 3$ , the phase transition is no longer described by conformal field theory (CFT) and exhibits continuously varying critical exponents (Fig. 2). Second, we determine the phase diagram associated with the transition as a function of the measurement rate  $p$  and the power-law exponent  $\alpha$  [Fig. 1(b)]. For  $\alpha > 2$ , the transition occurs between phases with volume- and

area-law scaling of entanglement entropy, while for  $\alpha < 2$ , the area-law entropy scaling crosses over to “subvolume” law scaling [56]. Finally, we develop an exact correspondence between hybrid quantum circuits with long-range interactions and a quantum Ising model with long-range interactions. This correspondence allows us to understand the measurement-induced transition in terms of the ground-state properties of a quantum spin chain [58–60]; perhaps most intriguingly, it provides an analytic explanation for the dramatic change in universality at  $\alpha \approx 3$ —this is precisely when long-range interactions become a relevant perturbation.

*Long-range hybrid quantum circuits.*—Consider a one-dimensional system of  $L$  qubits with periodic boundary conditions. Our hybrid quantum circuits consist of long-range gates interspersed with projective measurements [Fig. 1(a)] [61].

More precisely, a single time step of the *scrambling* portion of the evolution consists of  $L$  random two-qubit Clifford gates acting on qubits separated by  $r$  sites, with  $r$  sampled according to  $P(r) \sim 1/r^\alpha$ ; each scrambling time step is then followed by  $pL$  randomly placed projective measurements [56,62].

We have carefully chosen our scrambling dynamics to be qualitatively similar to those generated by long-range interacting Hamiltonians. Indeed, the light cone (as measured via an out-of-time-order correlator) for our random circuit model with power law  $\alpha$  is expected to match the corresponding light cone generated by *chaotic Hamiltonian* dynamics with power law  $\alpha/2$  [63]. To this end, our analysis also provides insights into the measurement-induced transition when the dynamics are driven by a long-range-interacting Hamiltonian (provided one maps  $\alpha \rightarrow \alpha/2$ ).

*Diagnostics.*—We characterize the dynamics of our long-range hybrid quantum circuits using four diagnostics: (i) the half-chain entanglement entropy ( $S_{L/2}$ ); (ii) the antipodal mutual information ( $I_{AB}$ ) [19,20]; (iii) the global purification dynamics ( $S(t)$ ) [26]; and (iv) the single-qubit purification time ( $\tau_p$ ) [27]. All observables are defined as average quantities over many circuit realizations, and  $S_{L/2}$  and  $I_{AB}$  are *steady-state* quantities, i.e., averaged over late times.

The half-chain entanglement entropy  $S_{L/2}$  is an intuitive diagnostic of the transition in the case of short-range interactions: at low measurement rates, the system evolves to an extensively entangled state and  $S_{L/2} \sim L$  (volume law), while at high measurement rates the system remains in a product state and  $S_{L/2} \sim O(1)$  (area law). Because of subleading corrections to its critical scaling form,  $S_{L/2}$  is challenging to work with quantitatively [19]. It turns out to be more straightforward to analyze  $I_{AB}$ , defined as the mutual information between two small anti-podal regions [Fig. 3(g)]. Crucially,  $I_{AB} \approx 0$  in both the product and extensively entangled phases (where the system is

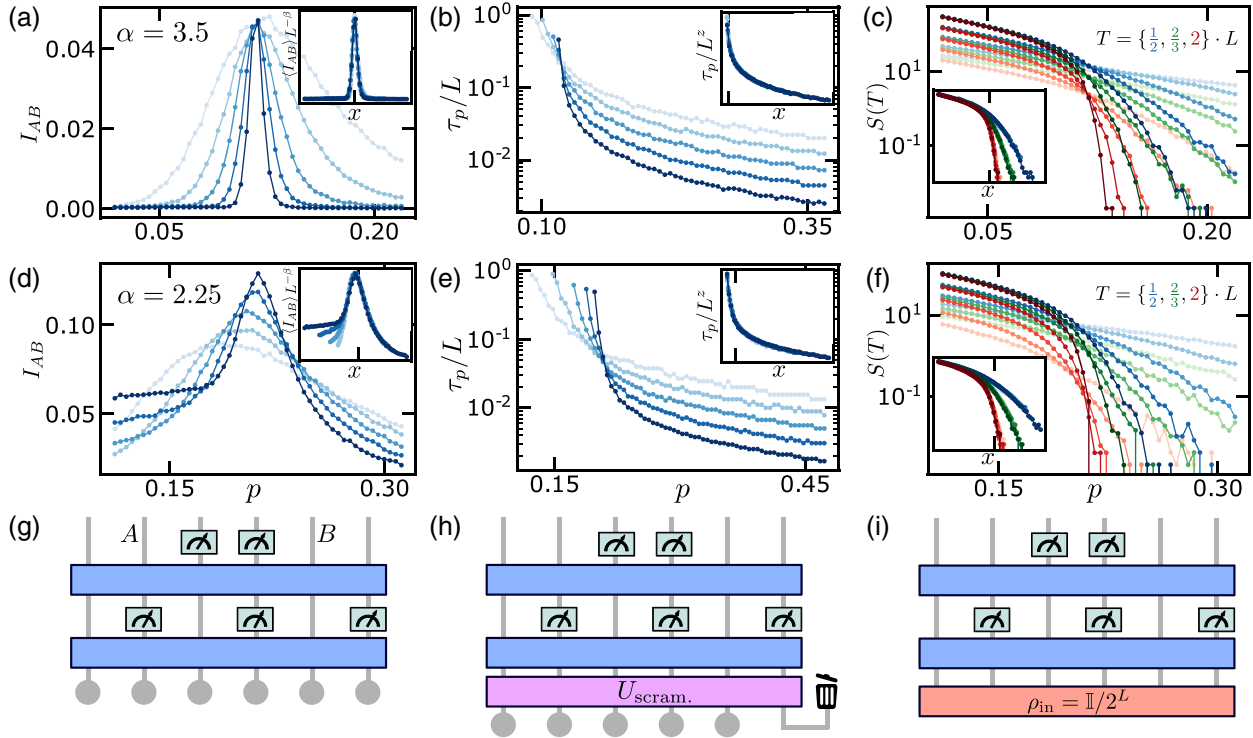


FIG. 3. (a)–(c) The antipodal mutual information  $I_{AB}$ , purification time  $\tau_p$ , and global entropy dynamics  $S(t)$  as a function of the measurement rate  $p$ , for power law  $\alpha = 3.5$ . Insets depict the corresponding finite-size scaling collapse with  $x = (p - p_c)L^{1/\nu}$  (the  $x$ -axis tick denotes  $x = 0$ ). Different system sizes ( $L = [32, 64, 128, 256, 512]$ ) are indicated via increasing opacity. (d)–(f) Depict analogous plots for  $\alpha = 2.25$ . Both the peak heights of  $I_{AB}$  [d] and the crossing points of  $\tau_p/L$  [e] exhibit marked  $L$  dependence. This immediately indicates that the measurement-induced transition is no longer conformal. (c), (f) Colors indicate different time slices of  $S(t)$  (see legend). Finite-size collapses (insets) are obtained by rescaling  $t = cL \rightarrow cL^z$ , with  $c = \{1/2, 2/3, 2\}$  depending on the time slice. (g) Circuit schematic for  $I_{AB}$ . The system is initialized in a product state and the mutual information is measured between antipodal regions  $A$  and  $B$ . (h) Circuit schematic for  $\tau_p$ . The system is initialized in a product state with a single maximally mixed qubit. To avoid early-time finite-size effects, we apply a global scrambling Clifford,  $U_s$ , before evolving with our hybrid circuit. (i) Circuit schematic for  $S(t)$ . The system is initialized in a maximally mixed state and slowly purifies under hybrid dynamics.

unentangled or thermal respectively), and only peaks in the critical region, making it simple to use for finite-size scaling [19].

Both  $S_{L/2}$  and  $I_{AB}$  require a notion of geometric locality to be well defined, which breaks down as  $\alpha \rightarrow 0$  [38,39]. Thus, in order to gain a complete understanding of the dynamics, we also consider  $\tau_p$ , the median time it takes for measurements to purify a single qubit [Fig. 3(h)] [27]. The qualitative physics of  $\tau_p$  can be understood by considering the fate of an initially localized bit of entropy (e.g., a single maximally mixed qubit). For high measurement rates, this bit of entropy remains localized and hence  $\tau_p$  is independent of system size and approaches a constant in the thermodynamic limit. Meanwhile, at low measurement rates, this bit of entropy becomes delocalized and is unlikely to purify, so  $\tau_p$  diverges with system size. At the critical point, we expect  $\tau_p \sim L^z$ , where  $z$  is the dynamical exponent. Finally, we complement our study of the median purification time by investigating the global entropy of an initially maximally mixed state as a function of time,  $S(t)$  [26]; indeed,  $\tau_p$  can be understood simply as

the half life of  $S(t)$ . For high measurement rates,  $S(t)$  decays exponentially, while for low measurement rates,  $S(t)$  becomes time independent.

*Long-range interactions with  $\alpha \gtrsim 3$ .*—As a starting point for our analysis, let us consider fixed  $\alpha = 3.5$ . The observables we investigate exhibit clear evidence of an entanglement phase transition at a critical measurement rate,  $p_c$  [Figs. 3(a)–3(c)]. Perhaps the most striking signature of the transition comes from the antipodal mutual information, which exhibits a peak at the critical point that sharpens with increasing system size [Fig. 3(a)]. Moreover, the height and location of this peak are independent of  $L$ , consistent with prior observations in short-range-interacting hybrid circuits [19]. This is a consequence of conformal symmetry at the critical point [19], and suggests that the measurement-induced transition remains a CFT for sufficiently weak power laws (Fig. 2). To quantitatively characterize the transition, we perform finite-size scaling [inset, Fig. 3(a)] using the scaling form

$$I_{AB} = L^\beta f[(p - p_c)L^{1/\nu}]. \quad (1)$$

Crucially, this allows us to extract both the scaling dimension  $\beta$  of  $I_{AB}$  and the correlation length exponent  $\nu$ . We find,  $\beta \approx 0$  and  $\nu \approx 1.3$  (Fig. 2), consistent with all prior results in short-range interacting models [19,20,26,28,65].

In order to extract the dynamical critical exponent, we turn to an analysis of the median purification time  $\tau_p$ . As shown in Fig. 3(b), we observe a *single* crossing point (which independently identifies  $p_c$ ) for  $\tau_p/L$  across all system sizes. This is consistent with the dynamical scaling hypothesis,

$$\tau_p(p) = L^z g[(p - p_c)L^{1/\nu}], \quad (2)$$

with  $z = 1$  (as expected for a CFT). The conformal nature of the transition is further confirmed by the finite-size-scaling collapse depicted in the inset of Fig. 3(b). A few remarks are in order. First, we find that the correlation length exponent extracted from  $\tau_p$  gives  $\nu \approx 1.3$ , in excellent agreement with both with the short-range transition and the scaling analysis of  $I_{AB}$  [56]. Second, one hopes that the critical exponents extracted from  $\tau_p$  can be used to directly collapse the full time dynamics of the global entropy  $S(t)$ . This is indeed born out by the data [Fig. 3(c)], where we have utilized the general scaling form,

$$S(p, t) = h[(p - p_c)L^{1/\nu}, t/L^z]. \quad (3)$$

Although we have focused our discussions on the specific case of  $\alpha = 3.5$ , an extensive numerical study of the transition for all  $\alpha \gtrsim 3$  reveals the same physics [56]. In particular, the critical exponents  $\nu$  and  $z$  are found to agree with their short-range values, implying that the universality class of the measurement-induced transition is unchanged for  $\alpha \gtrsim 3$ .

*Long-range interactions with  $\alpha \lesssim 3$ .*—We now turn our attention toward the new physics that arises for  $\alpha \lesssim 3$ . To be concrete, let us begin by applying the same diagnostic toolset to long-range hybrid circuits with  $\alpha = 2.25$ . Two profound differences emerge: (i) the location and height of the peak of  $I_{AB}$  drifts with system size [Fig. 3(d)], and (ii)  $\tau_p$  no longer exhibits a single crossing point [Fig. 3(e)]. These trends immediately imply  $\beta \neq 0$  and  $z \neq 1$ , indicating that sufficiently strong power laws alter the universality class of the transition. More specifically, the critical point is no longer described by CFT.

To determine precisely when the universality class of the transition changes, we extract  $\nu(\alpha)$  and  $z(\alpha)$  via the purification time and the collapse of  $S(t)$  [Figs. 3(e),3(f)] [66]. As shown in Fig. 2, for  $\alpha \lesssim 3$ , we find that  $\nu$  and  $z$  vary continuously; this identifies  $\alpha \approx 3$  as the threshold for which long-range effects become relevant for the measurement-induced transition.

Interestingly, further reducing  $\alpha$  yields additional modifications to the transition. Specifically, we find that for

$\alpha < 2$  the half-chain entanglement entropy always scales with system size even at very high measurement rate, i.e., there is no longer a true area-law phase. Instead, there is subvolume entropy scaling, where  $S_{L/2} \sim L^\mu$ , with  $0 < \mu < 1$  [56]. The emergence of this subvolume law scaling can be understood quite simply by analyzing the short-time half-chain entanglement generated by our dynamics. Indeed, a single layer of long-range gates contributes additional entropy  $\sim L^{2-\alpha}$  for  $\alpha < 2$ . Numerical analysis indicates this bound is approximately tight, and we conjecture  $\mu = 2 - \alpha$  [56]. We emphasize, however, that both the subvolume and area law regimes are in fact in the purifying phase, connected by a crossover, as evinced by the constant  $\tau_p$  at large measurement rate for  $\alpha < 2$  [56].

At  $\alpha = 1$ , the subvolume scaling becomes a true volume law, and the half-chain entanglement no longer probes the measurement-induced transition. However, observables that are not geometrically local, such as  $S(t)$ ,  $\tau_p$ , and the entangling power [39], do not suffer from this limitation and demonstrate that a measurement-induced transition occurs for all  $\alpha \geq 0$  [38,39].

*Effective quantum spin model.*—To provide a theoretical understanding for the change of universality at  $\alpha \approx 3$ , we develop a mapping that relates the steady-state entanglement entropy of our long-range hybrid quantum circuit to the ground-state properties of a long-range 1D quantum Ising model [56,67]. This mapping hinges on a conditional Rényi entropy (which is related to  $S_{L/2}$  via the replica method [68,69]),

$$S_A^{(2)} = -\log\left(\overline{\sum_m p_m^2 \text{tr} \rho_{A,m}^2}\right) + \log\left(\sum_m p_m^2\right), \quad (4)$$

where  $\bar{\cdot}$  represents an average over circuit realizations, and  $\rho_{A,m}$  is the reduced density matrix for subsystem  $A$ , conditioned on a specific set of measurement outcomes,  $m$ , with probabilities  $p_m$  [56,67]. Much like the half-chain entanglement entropy,  $S_A^{(2)}$  undergoes an area-law to volume-law transition as a function of the measurement rate [70,71]. Crucially, although this transition belongs to a different universality class, it is analytically tractable and will provide insights into the original transition.

In order to compute  $S_A^{(2)}$ , we consider a slightly modified circuit that trades random *connectivity* for random *interaction strengths*. To be precise, we consider a circuit consisting of layers of single-qubit Haar random unitaries, projective local- $Z$  measurements, and long-range Ising interactions  $\theta_{ij}Z_iZ_j$ , where  $\theta_{ij}$  are drawn from a Gaussian distribution with zero mean and variance  $\propto 1/|i-j|^\alpha$ . The scrambling properties of this circuit are similar to those in our original long-range circuit [Fig. 1(a)], and we believe that it undergoes a measurement-induced transition of the same universality class (as long as one considers the same observable).

One can calculate  $S_A^{(2)}$  for the modified circuit via an exact mapping to imaginary time evolution under a long-ranged Ising Hamiltonian [56,67]:

$$H_{\text{eff}} = -\sum_{ij} \frac{J}{|i-j|^\alpha} (3\sigma_i^z \sigma_j^z - \sigma_i^x \sigma_j^x) - \sum_i h\sigma_i^x. \quad (5)$$

In this context, the measurement-induced transition in  $S_A^{(2)}$  can be understood as the symmetry-breaking transition in the ground state of  $H_{\text{eff}}$  [67,72].

To this end, let us recall the effect of long-range interactions on the universality class of the Ising transition. In particular, one can consider the long-range tail as a perturbation to the action of the short-ranged model,  $\delta S = \int dq d\omega q^{\alpha-1} \phi_q \phi_{-q}$ , where  $q$  is the momentum,  $\omega$  is the Matsubara frequency, and  $\phi$  is the order parameter [58,73]. At the (short-ranged) Ising critical point, the scaling dimension of  $\delta S$  is  $3 - \alpha - \eta$ , where  $\eta/2$  is the scaling dimension of the order parameter. Thus, the long-range coupling becomes a relevant perturbation for the Ising transition when  $\alpha < 3 - \eta$ . This insight immediately allows us to understand why the measurement-induced transition's universality changes at  $\alpha \lesssim 3$ .

More precisely, we also expect long-range interactions to become relevant for the measurement-induced transition at  $\alpha = 3 - \eta$ , where  $\eta$  is now the anomalous dimension of the short-range measurement-induced transition. Although difficult to compute directly, one can estimate  $\eta$  in three ways: (i) in the modified circuit model from this section, the transition of  $S_A^{(2)}$  has  $\eta = 1/4$ , (ii) in a Haar-random hybrid circuit with infinite qudit dimension, the transition of  $S_{L/2}$  has  $\eta = 5/24$  (and is described by percolation), (iii) in numerics on short-range interacting hybrid Clifford circuits, one finds  $\eta \approx 0.22$  [28]. All of these calculations suggest  $\alpha \approx 2.8$  as the critical threshold for the relevance of long-range interactions, consistent with our numerical phase diagram (Fig. 2).

Our work opens the door to a number of intriguing future directions. First, it would be interesting to compare the critically purifying subvolume law phase obtained in Ref. [74] to the critical point of hybrid long-range circuits with  $\alpha < 2$ . Despite vastly different microscope origins, these fixed points both exhibit subvolume entanglement entropy scaling and polynomial purification time, hinting at the possibility of a common long-wavelength description. Second, our predicted phase diagram can be directly probed in current generation quantum simulators, including interacting boson [37,75] or trapped ion platforms [76]. The latter approach is particularly suitable because the long-range interaction can, in principle, be tuned between  $0 < \alpha < 3$  [77,78].

We gratefully acknowledge the insights of and discussions with Michael Gullans, Joel Moore, and Adam Nahum. We are particularly indebted to Chao-Ming Jian

for pointing out the anomalous dimension for hybrid circuits with infinite qudit dimension. This work was supported by multiple grants from the U.S. Department of Energy, including the Office of Science, Office of Advanced Scientific Computing Research, under the Accelerated Research in Quantum Computing (ARQC) program, the Office of Science, National Quantum Information Science Research Centers, Quantum Systems Accelerator (QSA) and the HEADS-QON project (Grant No. DE-SC0020376). M. B. acknowledges support through the Department of Defense (DOD) through the National Defense Science & Engineering Graduate (NDSEG) Fellowship Program. S. C. acknowledges support from the Miller Institute for Basic Research in Science. E. A. is supported in part by the Department of Energy Project No. DE-SC0019380 ‘‘The Geometry and Flow of Quantum Information: From Quantum Gravity to Quantum Technology’’ and by the Gyorgy Chair in Physics at UC Berkeley.

*Note added.*—Recently, we became aware of two complementary works on the measurement-induced transition in long-range interacting Hamiltonian systems [79,80], which also identify subvolume law phases.

- 
- [1] J. Preskill, *Quantum* **2**, 79 (2018).
  - [2] F. Arute *et al.*, *Nature (London)* **574**, 505 (2019).
  - [3] C. Gross and I. Bloch, *Science* **357**, 995 (2017).
  - [4] D. Bluvstein, A. Omran, H. Levine, A. Keesling, G. Semeghini, S. Ebadi, T. T. Wang, A. A. Michailidis, N. Maskara, W. W. Ho, S. Choi, M. Serbyn, M. Greiner, V. Vuletić, and M. D. Lukin, *Science* **371**, 1355 (2021).
  - [5] G. Semeghini, H. Levine, A. Keesling, S. Ebadi, T. T. Wang, D. Bluvstein, R. Verresen, H. Pichler, M. Kalinowski, R. Samajdar, A. Omran, S. Sachdev, A. Vishwanath, M. Greiner, V. Vuletic, and M. D. Lukin, *arXiv:2104.04119*.
  - [6] K. J. Satzinger *et al.*, *arXiv:2104.01180*.
  - [7] D. A. Abanin, E. Altman, I. Bloch, and M. Serbyn, *Rev. Mod. Phys.* **91**, 021001 (2019).
  - [8] R. Nandkishore and D. A. Huse, *Annu. Rev. Condens. Matter Phys.* **6**, 15 (2015).
  - [9] R. Vosk, D. A. Huse, and E. Altman, *Phys. Rev. X* **5**, 031032 (2015).
  - [10] J.-y. Choi, S. Hild, J. Zeiher, P. Schauß, A. Rubio-Abadal, T. Yefsah, V. Khemani, D. A. Huse, I. Bloch, and C. Gross, *Science* **352**, 1547 (2016).
  - [11] J. F. Poyatos, J. I. Cirac, and P. Zoller, *Phys. Rev. Lett.* **77**, 4728 (1996).
  - [12] B. Kraus, H. P. Büchler, S. Diehl, A. Kantian, A. Micheli, and P. Zoller, *Phys. Rev. A* **78**, 042307 (2008).
  - [13] S. Shankar, M. Hatridge, Z. Leghtas, K. M. Sliwa, A. Narla, U. Vool, S. M. Girvin, L. Frunzio, M. Mirrahimi, and M. H. Devoret, *Nature (London)* **504**, 419 (2013).
  - [14] I. Carusotto, A. A. Houck, A. J. Kollár, P. Roushan, D. I. Schuster, and J. Simon, *Nat. Phys.* **16**, 268 (2020).
  - [15] X. Q. Shao, J. H. Wu, X. X. Yi, and G.-L. Long, *Phys. Rev. A* **96**, 062315 (2017).

- [16] We note a different model consisting *only* of noncommuting measurements [17] also demonstrates an entanglement transition.
- [17] M. Ippoliti, M. J. Gullans, S. Gopalakrishnan, D. A. Huse, and V. Khemani, *Phys. Rev. X* **11**, 011030 (2021).
- [18] Y. Li, X. Chen, and M. P. A. Fisher, *Phys. Rev. B* **98**, 205136 (2018).
- [19] Y. Li, X. Chen, and M. P. A. Fisher, *Phys. Rev. B* **100**, 134306 (2019).
- [20] B. Skinner, J. Ruhman, and A. Nahum, *Phys. Rev. X* **9**, 031009 (2019).
- [21] A. Chan, R. M. Nandkishore, M. Pretko, and G. Smith, *Phys. Rev. B* **99**, 224307 (2019).
- [22] S. Choi, Y. Bao, X.-L. Qi, and E. Altman, *Phys. Rev. Lett.* **125**, 030505 (2020).
- [23] H. Carmichael, *An Open Systems Approach to Quantum Optics: Lectures Presented at the Université libre de Bruxelles*, Lecture Notes in Physics No. m18 (Springer-Verlag, Berlin; New York, 1993).
- [24] C. Gardiner and P. Zoller, *Quantum Noise: A Handbook of Markovian and Non-Markovian Quantum Stochastic Methods with Applications to Quantum Optics*, 3rd ed., Springer Series in Synergetics (Springer-Verlag, Berlin Heidelberg, 2004).
- [25] A. A. Clerk, M. H. Devoret, S. M. Girvin, F. Marquardt, and R. J. Schoelkopf, *Rev. Mod. Phys.* **82**, 1155 (2010).
- [26] M. J. Gullans and D. A. Huse, *Phys. Rev. X* **10**, 041020 (2020).
- [27] M. J. Gullans and D. A. Huse, *Phys. Rev. Lett.* **125**, 070606 (2020).
- [28] A. Zabalo, M. J. Gullans, J. H. Wilson, S. Gopalakrishnan, D. A. Huse, and J. H. Pixley, *Phys. Rev. B* **101**, 060301(R) (2020).
- [29] Y. Li and M. P. A. Fisher, *Phys. Rev. B* **103**, 104306 (2021).
- [30] M. J. Gullans and D. A. Huse, *Phys. Rev. Lett.* **123**, 110601 (2019).
- [31] R. Fan, S. Vijay, A. Vishwanath, and Y.-Z. You, *Phys. Rev. B* **103**, 174309 (2021).
- [32] R. Vasseur, A. C. Potter, Y.-Z. You, and A. W. W. Ludwig, *Phys. Rev. B* **100**, 134203 (2019).
- [33] A. Lavasani, Y. Alavirad, and M. Barkeshli, *Nat. Phys.* **17**, 342 (2021).
- [34] X. Cao, A. Tilloy, and A. De Luca, *SciPost Phys.* **7**, 024 (2019).
- [35] M. J. Gullans and D. A. Huse, *Phys. Rev. X* **9**, 021007 (2019).
- [36] M. Szyniszewski, A. Romito, and H. Schomerus, *Phys. Rev. B* **100**, 064204 (2019).
- [37] Q. Tang and W. Zhu, *Phys. Rev. Research* **2**, 013022 (2020).
- [38] A. Nahum, S. Roy, B. Skinner, and J. Ruhman, *PRX Quantum* **2**, 010352 (2021).
- [39] S. Vijay, *arXiv:2005.03052*.
- [40] L. Piroli, C. Sünderhauf, and X.-L. Qi, *J. High Energy Phys.* **04** (2020) 063.
- [41] D. J. Thouless, *Phys. Rev.* **187**, 732 (1969).
- [42] N. D. Mermin and H. Wagner, *Phys. Rev. Lett.* **17**, 1133 (1966).
- [43] P. C. Hohenberg, *Phys. Rev.* **158**, 383 (1967).
- [44] M. F. Maghrebi, Z.-X. Gong, and A. V. Gorshkov, *Phys. Rev. Lett.* **119**, 023001 (2017).
- [45] B. S. Shastry, *Phys. Rev. Lett.* **60**, 639 (1988).
- [46] F. D. M. Haldane, *Phys. Rev. Lett.* **60**, 635 (1988).
- [47] M. C. Tran, C.-F. Chen, A. Ehrenberg, A. Y. Guo, A. Deshpande, Y. Hong, Z.-X. Gong, A. V. Gorshkov, and A. Lucas, *Phys. Rev. X* **10**, 031009 (2020).
- [48] X. Chen and T. Zhou, *Phys. Rev. B* **100**, 064305 (2019).
- [49] C.-F. Chen and A. Lucas, *Phys. Rev. Lett.* **123**, 250605 (2019).
- [50] D. V. Else, F. Machado, C. Nayak, and N. Y. Yao, *Phys. Rev. A* **101**, 022333 (2020).
- [51] M. Saffman, T. G. Walker, and K. Mølmer, *Rev. Mod. Phys.* **82**, 2313 (2010).
- [52] D. DeMille, *Phys. Rev. Lett.* **88**, 067901 (2002).
- [53] C. Monroe, W. C. Campbell, L.-M. Duan, Z.-X. Gong, A. V. Gorshkov, P. W. Hess, R. Islam, K. Kim, N. M. Linke, G. Pagano, P. Richerme, C. Senko, and N. Y. Yao, *Rev. Mod. Phys.* **93**, 025001 (2021).
- [54] E. J. Davis, B. Ye, F. Machado, S. A. Meynell, T. Mittiga, W. Schenken, M. Joos, B. Kobrin, Y. Lyu, D. Bluvstein, S. Choi, C. Zu, A. C. B. Jayich, and N. Y. Yao, *arXiv:2103.12742*.
- [55] L. T. Hall, P. Kehayias, D. A. Simpson, A. Jarmola, A. Stacey, D. Budker, and L. C. L. Hollenberg, *Nat. Commun.* **7**, 10211 (2016).
- [56] See Supplemental Material at <http://link.aps.org/supplemental/10.1103/PhysRevLett.128.010604> for additional information, which includes Ref. [57].
- [57] B. Collins, *Int. Math. Res. Not.* **2003**, 953 (2003).
- [58] J. Sak, *Phys. Rev. B* **8**, 281 (1973).
- [59] A. Dutta and J. K. Bhattacharjee, *Phys. Rev. B* **64**, 184106 (2001).
- [60] N. Defenu, A. Trombettoni, and S. Ruffo, *Phys. Rev. B* **96**, 104432 (2017).
- [61] We employ Clifford gates to make the simulation of large system systems practically feasible. The dynamics of random Clifford circuits are qualitatively similar to those of Haar-random circuits [28].
- [62] Other few-body measurements, such as two-qubit parity measurements, result in an equivalent model [17].
- [63] To summarize the argument given in Ref. [64]: operator spreading in chaotic dynamics is determined by a local coupling strength  $J$  and a local decoherence time  $\tau$ , with operator spreading occurring at a rate  $J^2/\tau$ . If  $J1/r^\alpha$ , then the random circuit model with similar operator-spreading properties should have power-law exponent  $2\alpha$ .
- [64] T. Zhou, S. Xu, X. Chen, A. Guo, and B. Swingle, *Phys. Rev. Lett.* **124**, 180601 (2020).
- [65] In fact, in the short-range case  $\beta = 0$  is fixed by conformal symmetry in space-time, but we do not assume any symmetry here.
- [66] We use  $\tau_p$  rather than  $I_{AB}$  because the latter is an inaccurate quantitative probe of the transition for  $\alpha < 3$ ; see Ref. [56].
- [67] Y. Bao, S. Choi, and E. Altman, *Ann. Phys. (Amsterdam)* **168618** (2021).
- [68] P. Hayden, S. Nezami, X.-L. Qi, N. Thomas, M. Walter, and Z. Yang, *J. High Energy Phys.* **11** (2016) 009.
- [69] A. Nahum, S. Vijay, and J. Haah, *Phys. Rev. X* **8**, 021014 (2018).
- [70] Y. Bao, S. Choi, and E. Altman, *Phys. Rev. B* **101**, 104301 (2020).

- [71] C.-M. Jian, Y.-Z. You, R. Vasseur, and A. W. W. Ludwig, *Phys. Rev. B* **101**, 104302 (2020).
- [72] For  $\alpha < 1$ , the requirement that the original circuit has only  $L$  gates per time step results in renormalized couplings in the Hamiltonian model,  $J \rightarrow J/L^{1-\alpha}$ , so that it remains thermodynamically stable.
- [73] M. E. Fisher, S.-K. Ma, and B. G. Nickel, *Phys. Rev. Lett.* **29**, 917 (1972).
- [74] M. Ippoliti, T. Rakovszky, and V. Khemani, [arXiv:2103.06873](https://arxiv.org/abs/2103.06873).
- [75] C.-L. Hung, A. González-Tudela, J. I. Cirac, and H. J. Kimble, *Proc. Natl. Acad. Sci. U.S.A.* **113**, E4946 (2016).
- [76] C. Noel, P. Niroula, A. Risinger, L. Egan, D. Biswas, M. Cetina, A. V. Gorshkov, M. Gullans, D. A. Huse, and C. Monroe, [arXiv:2106.05881](https://arxiv.org/abs/2106.05881).
- [77] D. Porras and J. I. Cirac, *Phys. Rev. Lett.* **92**, 207901 (2004).
- [78] G. Pagano, A. Bapat, P. Becker, K. S. Collins, A. De, P. W. Hess, H. B. Kaplan, A. Kyprianidis, W. L. Tan, C. Baldwin *et al.*, *Proc. Natl. Acad. Sci. U.S.A.* **117**, 25396 (2020).
- [79] T. Minato, K. Sugimoto, T. Kuwahara, and K. Saito, preceding Letter, *Phys. Rev. Lett.* **128**, 010603 (2022).
- [80] T. Müller, S. Diehl, and M. Buchhold, following Letter, *Phys. Rev. Lett.* **128**, 010605 (2022).